Haar wavelets on spherical triangulations

Daniela Roşca

University of Lübeck, Institute of Mathematics, Wallstrasse 40, 23560 Lübeck, Germany
and
Technical University of Cluj-Napoca, Dept. of Mathematics, str. Daicoviciu 15, 400020, Cluj-Napoca, Romania
Daniela.Catinas@math.utcluj.ro

Abstract
We construct piecewise constant wavelets on spherical triangulations, which are orthogonal with respect to a scalar product on $L^2(\mathbb{S}^2)$, defined in [3]. Our classes of wavelets include the wavelets obtained by Bonneau in [1] and by Nielson et all. in [2]. We also proved the Riesz stability and showed some numerical experiments.

1 Introduction

In [1] and [2] some "nearly orthogonal" piecewise constant wavelets defined on arbitrary triangulations of the sphere $\mathbb{S}^2$ of $\mathbb{R}^3$ are presented. In [2] a spherical wavelet basis is said to be *nearly orthogonal* if it becomes orthogonal when the subdivision depth increases (i.e. when the spherical triangles are "near" planar). Actually, the orthogonality occurs if, at each level of the multiresolution, the areas of the spherical triangles are approximated with the areas of the corresponding planar triangles. Some numerical examples show that this idea works well in practice, but no mathematical arguments were given to assure that it works in practice all the time.

In this paper we use a scalar product $\langle \cdot, \cdot \rangle_*$ on $L^2\left(\mathbb{S}^2\right)$, defined in [3], which induces a norm $\|\cdot\|_*$ equivalent to the usual 2-norm of $L^2\left(\mathbb{S}^2\right)$. Then we construct piecewise constant wavelets which are orthogonal with respect to this scalar product. The equivalence of the norms $\|\cdot\|_*$ and the usual 2-norm of $L^2\left(\mathbb{S}^2\right)$ will help us to prove the Riesz stability in $L^2\left(\mathbb{S}^2\right)$ of our wavelets.

2 Preliminaries

Consider the unit sphere $\mathbb{S}^2$ of $\mathbb{R}^3$ with the center in O and Π a convex polyhedron having triangular faces[1] and the vertices situated on the sphere. Also we have to suppose that no face contains the origin O and O is situated inside the polyhedron. We denote by $\mathcal{T}^0 = \{T_1, T_2, \ldots, T_n\}$ the set of the faces of Π and by Ω the surface (the "cover") of Π. Then we consider the radial projection onto $\mathbb{S}^2$, $p : \Omega \to \mathbb{S}^2$,

$$p(x, y, z) = \frac{1}{\sqrt{x^2 + y^2 + z^2}} (x, y, z), \ (x, y, z) \in \Omega \tag{1}$$

and its inverse $p^{-1} : \mathbb{S}^2 \to \Omega$,

$$p^{-1}(\eta_1, \eta_2, \eta_3) = \frac{-d}{a\eta_1 + b\eta_2 + c\eta_3} (\eta_1, \eta_2, \eta_3), \ (\eta_1, \eta_2, \eta_3) \in \mathbb{S}^2,$$

where $ax + by + cz + d = 0$ is the equation of the face of Π onto which the point $(\eta_1, \eta_2, \eta_3) \in \mathbb{S}^2$ projects. In case this projection is situated on an edge, then one of the two faces containing that edge is taken.

Being given Ω, we can say that $\mathcal{T} = \mathcal{T}^0$ is a triangulation of Ω. Next we wish to consider its uniform refinement $\mathcal{T}^1$. For a given triangle $[M_1M_2M_3]$ in $\mathcal{T}^0$, let A_1, A_2, A_3 denote the midpoints of the edges M_2M_3, M_3M_1 and M_1M_2, respectively. Then we consider the set

$$\mathcal{T}^1 = \bigcup_{[M_1M_2M_3] \in \mathcal{T}^0} \{[M_1A_2A_3], [A_1M_2A_3], [A_1A_2M_3], [A_1A_2A_3]\},$$

which is also a triangulation of Ω. Proceeding in the same way the refinement process we can obtain a triangulation $\mathcal{T}^j$ of Ω, for $j \in \mathbb{N}$. The projection of $\mathcal{T}^j$ onto the sphere will be $\mathcal{U}^j = \left\{p\left(T^j\right), \ T^j \in \mathcal{T}^j\right\}$, which is a triangulation of $\mathbb{S}^2$. The number of triangles in $\mathcal{U}^j$ will be $\left|\mathcal{U}^j\right| = n \cdot 4^j$.

Let $\langle \cdot, \cdot \rangle_\Omega$ be the following inner product, based on the initial coarsest triangulation $\mathcal{T}^0$:

$$\langle f, g \rangle_\Omega = \sum_{T \in \mathcal{T}^0} \frac{1}{a(T)} \int_T f(\mathbf{x}) g(\mathbf{x}) \, d\mathbf{x}, \ \text{ for } f, g \in C(T) \ \forall T \in \mathcal{T}^0.$$

Here $a(T)$ denotes the area of the triangle T. Also, we consider the induced norm

$$\|f\|_\Omega = \langle f, f \rangle_\Omega^{1/2}.$$

For the L^2-integrable functions F and G defined on $\mathbb{S}^2$, the following scalar product associated to the given polyhedron Π was defined in [3]:

[1] The polyhedron could also have faces which are not triangles. In this case we triangulate each of these faces and consider it as having triangular faces, with some of the faces coplanar triangles.

$$\langle F, G\rangle_* = \langle F\circ p, G\circ p\rangle_\Omega . \tag{2}$$

There it was proved that, in the space $L^2\left(\mathbb{S}^2\right)$, the norm $\|\cdot\|_*$ induced by this scalar product is equivalent to the usual norm $\|\cdot\|_{L^2(\mathbb{S}^2)}$ of $L^2\left(\mathbb{S}^2\right)$ and

$$m\,\|F\|^2_{L^2(\mathbb{S}^2)} \le \|F\|^2_* \le M\,\|F\|^2_{L^2(\mathbb{S}^2)}\,, \tag{3}$$

with $m = \frac{1}{4}\min\limits_{T\in\mathcal{T}^0}\frac{d_T^2}{a(T)^3}$, $M = 2\max\limits_{T\in\mathcal{T}^0}\frac{1}{|d_T|}$, $d_T = \begin{vmatrix} x_1 & y_1 & z_1 \\ x_2 & y_2 & z_2 \\ x_3 & y_3 & z_3 \end{vmatrix}$, for each triangle T having the vertices $B_i\left(x_i, y_i, z_i\right)$, $i = 1, 2, 3$. If we use the relation $|d_T| = 2a\left(T\right)\operatorname{dist}\left(O, T\right)$, with $\operatorname{dist}\left(O, T\right)$ representing the distance from the origin to the plane of the triangle T, then the values m and M become

$$m = \min_{T\in\mathcal{T}^0}\frac{\operatorname{dist}^2\left(O,T\right)}{a\left(T\right)},$$
$$M = \max_{T\in\mathcal{T}^0}\frac{1}{a\left(T\right)\operatorname{dist}\left(O,T\right)}.$$

In the following we construct a multiresolution on $\mathbb{S}^2$ consisting of piecewise constant functions on the triangles of $\mathcal{U}^j = \left\{U_1^j, U_2^j, \ldots, U_{n\cdot 4^j}^j\right\}$, $j\in\mathbb{N}$.

By definition, a multiresolution of $L^2\left(\mathbb{S}^2\right)$ is a sequence of subspaces $\left\{V^j : j\ge 0\right\}$ of $L^2\left(\mathbb{S}^2\right)$ which satisfies the following properties:

1. $V^j \subseteq V^{j+1}$ for all $j\in\mathbb{N}$,
2. $\operatorname{clos}_{L^2(\mathbb{S}^2)}\bigcup\limits_{j=0}^{\infty} V^j = L^2\left(\mathbb{S}^2\right)$,
3. There are index sets $\mathcal{K}_j \subseteq \mathcal{K}_{j+1}$ such that for every level j there exists a Riesz basis $\left\{\varphi_t^j,\ t\in\mathcal{K}_j\right\}$ of the space V^j. This means that there exist constants $0 < c < C < \infty$, independent of the level j, such that

$$c2^{-j}\left\|\left\{c_t^j\right\}_{t\in\mathcal{K}^j}\right\|_{l_2(\mathcal{K}_j)} \le \left\|\sum_{t\in\mathcal{K}^j} c_t^j\varphi_t^j\right\|_{L^2(\mathbb{S}^2)} \le C2^{-j}\left\|\left\{c_t^j\right\}_{t\in\mathcal{K}^j}\right\|_{l_2(\mathcal{K}_j)}.$$

3 The spaces V^j and W^j

For a fixed $j\in\mathbb{N}$, to each triangle $U_k^j\in\mathcal{U}^j$, $k = 1, 2, \ldots, n\cdot 4^j$, we associate the function $\varphi_{U_k^j} : \mathbb{S}^2 \to \mathbb{R}$,

$$\varphi_{U_k^j}\left(\eta\right) = \begin{cases} 1, & \text{inside the triangle } U_k^j\,, \\ 1/2, & \text{on the edges of } U_k^j\,, \\ 0, & \text{in rest.} \end{cases}$$

Then we define the spaces of functions $V^j = \text{span}\left\{\varphi_{U_k^j},\ k = 1, 2, \ldots, n \cdot 4^j\right\}$, consisting of piecewise constant functions on the triangles of $\mathcal{U}^j$.

It is immediate that the set $\left\{\varphi_{U_k^j},\ k = 1, 2, \ldots, n \cdot 4^j\right\}$ is a basis for V^j, so $\left|V^j\right| = n \cdot 4^j$.

We must establish the relation between the spaces V^j and V^{j+1}. Let $U^j \in \mathcal{U}^j$ and $U_k^{j+1} = p\left(T_k^{j+1}\right)$, $k = 1, 2, 3, 4$, the refined triangles obtained from U^j, as in Figure 1.

We have

$$\varphi_{U^j} = \varphi_{U_1^{j+1}} + \varphi_{U_2^{j+1}} + \varphi_{U_3^{j+1}} + \varphi_{U_4^{j+1}},$$

equality which holds in $L^2\left(\mathbb{S}^2\right)$. Thus, $V^j \subseteq V^{j+1}$ for all $j \in \mathbb{N}$. With respect to the scalar product $\langle \cdot, \cdot \rangle_*$, the spaces V^j and V^{j+1} become Hilbert spaces, with the corresponding norm $\|\cdot\|_* = \langle \cdot, \cdot \rangle^{1/2}$.

Next we define the space W^j as the orthogonal complement, with respect to the scalar product $\langle \cdot, \cdot \rangle_*$, of the coarse space V^j in the fine space V^{j+1} :

$$V^{j+1} = V^j \bigoplus W^j.$$

The spaces W^j are called *the wavelet spaces.* The dimension of W^j is $\left|W^j\right| = \left|V^{j+1}\right| - \left|V^j\right| = 3n \cdot 4^j$.

In the following we will construct a basis of W^j. Let us take the triangle U^j and its refinements U_1^{j+1}, U_2^{j+1}, U_3^{j+1}, U_4^{j+1} and denote $F_{U^j}^1$, $F_{U^j}^2$, $F_{U^j}^3$ the projections onto $\mathbb{S}^2$ of the mid-points of the edges of the plane triangle $p^{-1}\left(U^j\right)$, as in Figure 1.

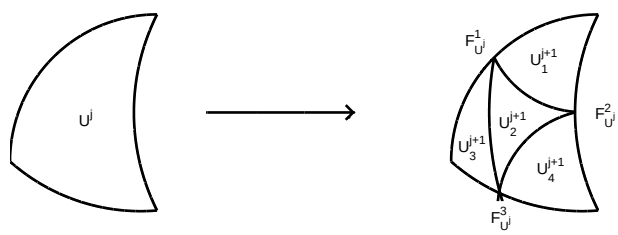

Fig. 1. The triangle U^j and its refined triangles U_k^{j+1}, $k = 1, 2, 3, 4$.

Note that, except for the case $j = 0$, the points $F_{U^j}^l$, $l = 1, 2, 3$, are not in general mid-points of the edges of the spherical triangle U^j. To each of these points $F_{U^j}^l$ a wavelet will be associated in the following way

$$\begin{aligned}
\Psi_{F_{j+1}^1, U^j} &= \alpha_1 \varphi_{U_1^{j+1}} + \alpha_2 \varphi_{U_3^{j+1}} + \beta \varphi_{U_2^{j+1}} + \gamma \varphi_{U_4^{j+1}}, \\
\Psi_{F_{j+1}^2, U^j} &= \alpha_1 \varphi_{U_4^{j+1}} + \alpha_2 \varphi_{U_1^{j+1}} + \beta \varphi_{U_2^{j+1}} + \gamma \varphi_{U_3^{j+1}}, \\
\Psi_{F_{j+1}^3, U^j} &= \alpha_1 \varphi_{U_3^{j+1}} + \alpha_2 \varphi_{U_4^{j+1}} + \beta \varphi_{U_2^{j+1}} + \gamma \varphi_{U_1^{j+1}},
\end{aligned} \tag{4}$$

with $\alpha_1, \alpha_2, \beta, \gamma \in \mathbb{R}$. Let us mention that supp $\Psi_{F^k_{j+1},U^j} = U^j$ for $k = 1, 2, 3$.

Next we will find conditions on the coefficients $\alpha_1, \alpha_2, \beta, \gamma$, which assure that the set

$$\left\{\Psi_{F^k_{j+1},U^j},\ k = 1, 2, 3,\ U^j \in \mathcal{U}^j\right\}$$

is an orthonormal basis of W^j with respect to the scalar product defined in (2).

First we must have

$$\left\langle \Psi_{F^k_{j+1},U^j}, \varphi_{S^j} \right\rangle_* = 0, \tag{5}$$

for $k = 1, 2, 3$ and $U^j,\ S^j \in \mathcal{U}^j$. If $U^j \neq S^j$, then the equality is immediate since supp $\Psi_{F^k_{j+1},U^j}$ = supp φ_{U^j} and supp $\varphi_{S^j} \cap$ supp φ_{U^j} is either the $\emptyset$ or an edge, whose measure is zero. For $U^j = S^j$, evaluating the scalar product (5) we obtain

$$\left\langle \Psi_{F^1_{j+1},U^j}, \varphi_{S^j} \right\rangle_* = \frac{\alpha_1 \mathcal{A}_1^{j+1} + \alpha_2 \mathcal{A}_3^{j+1} + \beta \mathcal{A}_2^{j+1} + \gamma \mathcal{A}_4^{j+1}}{a\left(p^{-1}\left(U\right)\right)},$$

U being the triangle of the initial triangulation $\mathcal{U}^0$ which includes the triangle U^j and $\mathcal{A}_k^{j+1} = a\left(p^{-1}\left(U_k^{j+1}\right)\right)$. Since

$$\frac{\mathcal{A}_k^{j+1}}{a\left(p^{-1}\left(U\right)\right)} = 4^{-(j+1)} \text{ for } k = 1, 2, 3, 4,$$

the orthogonality conditions (5) reduce to

$$\alpha_1 + \alpha_2 + \beta + \gamma = 0. \tag{6}$$

Now we have to find conditions on the parameters $\alpha_1, \alpha_2, \beta, \gamma$ such that the functions $\left\{\Psi_{F^k_{j+1},U^j},\ k = 1, 2, 3,\ U^j \in \mathcal{U}^j\right\}$ are linearly independent. Let $\lambda_{F^1,U^j}, \lambda_{F^2,U^j}, \lambda_{F^3,U^j} \in \mathbb{R}$ for $U^j \in \mathcal{U}^j$. Taking the linear combination

$$\sum_{k=1}^{3} \sum_{U^j \in \mathcal{U}^j} \lambda_{F^k,U^j} \Psi_{F^k_{j+1},U^j} = 0,$$

it follows that for each $U^j \in \mathcal{U}^j$ we must have

$$\sum_{k=1}^{3} \lambda_{F^k,U^j} \Psi_{F^k_{j+1},U^j} = 0. \tag{7}$$

In order to simplify the writing we denote $\lambda_{F^k,U^j} = \lambda_k$. The linear independency occurs if each relation (7) implies $\lambda_1 = \lambda_2 = \lambda_3 = 0$. Using the definitions (4) we obtain

$$\begin{aligned}\lambda_1\alpha_1+\lambda_2\alpha_2+\lambda_3\gamma&=0,\\ \lambda_1\beta+\lambda_2\beta+\lambda_3\beta&=0,\\ \lambda_1\alpha_2+\lambda_2\gamma+\lambda_3\alpha_1&=0,\\ \lambda_1\gamma+\lambda_2\alpha_1+\lambda_3\alpha_2&=0.\end{aligned}$$

Taking into account the condition (6) , we can deduce that this system of 4 equations with 3 unknowns has only the zero solution if and only if

$$\alpha_1^3+\alpha_2^3+\gamma^3-3\alpha_1\alpha_2\gamma\neq 0. \tag{8}$$

So, if this condition is satisfied, then a basis in W^j is constructed.

Now we want to look for an orthogonal basis. Each of the orthogonality conditions

$$\left\langle \Psi_{F^k_{j+1},U^j},\Psi_{F^l_{j+1},U^j}\right\rangle_*=0$$

for $l,k\in\{1,2,3\}$, $l\neq k$ and $U^j\in\mathcal{U}^j$ is equivalent to

$$\alpha_1\alpha_2+(\alpha_1+\alpha_2)\,\gamma+\beta^2=0. \tag{9}$$

Solving the system consisting of the equations (6) and (9) we get

$$\beta^2-(\alpha_1+\alpha_2)\,\beta-\left(\alpha_1^2+\alpha_1\alpha_2+\alpha_2^2\right)=0. \tag{10}$$

We wish to have orthonormal bases, so we impose the condition

$$\left\|2^j\cdot\Psi_{F^l_{j+1},U^j}\right\|_*=1\quad\text{for } l=1,2,3.$$

Using the relations (6) and (10) we obtain, for $l=1,2,3$,

$$\left\|2^j\cdot\Psi_{F^l_{j+1},\ U^j}\right\|_*=\alpha_1^2+\alpha_2^2+\beta^2+\gamma^2=4\beta^2.$$

Hence, $\beta=\pm\frac{1}{2}$.

For $\beta=\frac{1}{2}$ condition (10) reduces to

$$4\left(\alpha_1^2+\alpha_1\alpha_2+\alpha_2^2\right)+2\left(\alpha_1+\alpha_2\right)-1=0$$

and condition (8) reduces to

$$2\left(\alpha_1^2+\alpha_1\alpha_2+\alpha_2^2\right)+\left(\alpha_1+\alpha_2\right)\neq 0.$$

The small ellipse, having the equation $2\left(\alpha_1^2+\alpha_1\alpha_2+\alpha_2^2\right)+\left(\alpha_1+\alpha_2\right)=0$, contains the points (α_1,α_2) for which the wavelets become linearly dependent. In conclusion, there exist orthogonal wavelets for all (α_1,α_2) situated on the big ellipse plotted in Figure 2. These wavelets have the expression

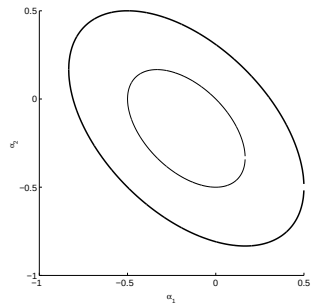

Fig. 2. The graph of the curve $4\left(\alpha_1^2+\alpha_1\alpha_2+\alpha_2^2\right)+2\left(\alpha_1+\alpha_2\right)-1=0$ (the big ellipse), resp. $2\left(\alpha_1^2+\alpha_1\alpha_2+\alpha_2^2\right)+\left(\alpha_1+\alpha_2\right)=0$ (the small ellipse).

$$
\begin{aligned}
{}^1\Psi_{F^1_{j+1},U^j} &= \alpha_1\varphi_{U_1^{j+1}}+\alpha_2\varphi_{U_3^{j+1}}+\frac{1}{2}\varphi_{U_2^{j+1}}-\left(\frac{1}{2}+\alpha_1+\alpha_2\right)\varphi_{U_4^{j+1}},\\
{}^1\Psi_{F^2_{j+1},U^j} &= \alpha_1\varphi_{U_4^{j+1}}+\alpha_2\varphi_{U_1^{j+1}}+\frac{1}{2}\varphi_{U_2^{j+1}}-\left(\frac{1}{2}+\alpha_1+\alpha_2\right)\varphi_{U_3^{j+1}},\\
{}^1\Psi_{F^3_{j+1},U^j} &= \alpha_1\varphi_{U_3^{j+1}}+\alpha_2\varphi_{U_4^{j+1}}+\frac{1}{2}\varphi_{U_2^{j+1}}-\left(\frac{1}{2}+\alpha_1+\alpha_2\right)\varphi_{U_1^{j+1}}.
\end{aligned}
$$

For $\beta=-\frac{1}{2}$ condition (10) reduces to

$$4\left(\alpha_1^2+\alpha_1\alpha_2+\alpha_2^2\right)-2\left(\alpha_1+\alpha_2\right)-1=0,$$

while condition (8) reduces to

$$2\left(\alpha_1^2+\alpha_1\alpha_2+\alpha_2^2\right)-\left(\alpha_1+\alpha_2\right)\neq 0.$$

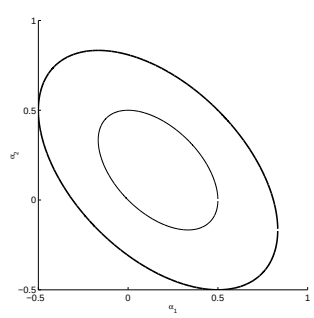

Fig. 3. The graphic of the curve $4\left(\alpha_1^2+\alpha_1\alpha_2+\alpha_2^2\right)-2\left(\alpha_1+\alpha_2\right)-1=0$ (the big ellipse), resp. $2\left(\alpha_1^2+\alpha_1\alpha_2+\alpha_2^2\right)-\left(\alpha_1+\alpha_2\right)=0$ (the small ellipse)

Again, there exist orthogonal wavelets for all (α_1,α_2) situated on the big ellipse plotted in Figure 3. These wavelets have the expression

$$
\begin{aligned}
{}^2\Psi_{F^1_{j+1},U^j} &= \alpha_1\varphi_{U^{j+1}_1} + \alpha_2\varphi_{U^{j+1}_3} - \frac{1}{2}\varphi_{U^{j+1}_2} + \left(\frac{1}{2} - \alpha_1 - \alpha_2\right)\varphi_{U^{j+1}_4},\\
{}^2\Psi_{F^2_{j+1},U^j} &= \alpha_1\varphi_{U^{j+1}_4} + \alpha_2\varphi_{U^{j+1}_1} - \frac{1}{2}\varphi_{U^{j+1}_2} + \left(\frac{1}{2} - \alpha_1 - \alpha_2\right)\varphi_{U^{j+1}_3},\\
{}^2\Psi_{F^3_{j+1},U^j} &= \alpha_1\varphi_{U^{j+1}_3} + \alpha_2\varphi_{U^{j+1}_4} - \frac{1}{2}\varphi_{U^{j+1}_2} + \left(\frac{1}{2} - \alpha_1 - \alpha_2\right)\varphi_{U^{j+1}_1}.
\end{aligned}
$$

Let us remark that if we choose $\alpha_1 = \alpha_2 = \alpha$, then we obtain the families of wavelets $\left\{{}^1\Psi^1_{F^l_{j+1},U^j}\right\}$, $\left\{{}^1\Psi^2_{F^l_{j+1},U^j}\right\}$, $\left\{{}^2\Psi^1_{F^l_{j+1},U^j}\right\}$ and $\left\{{}^2\Psi^2_{F^l_{j+1},U^j}\right\}$, given by

$$
\begin{aligned}
{}^1\Psi^1_{F^l_{j+1},\,U^j} &= -\frac{1}{2}\left(\varphi_{U^{j+1}_1} + \varphi_{U^{j+1}_3} - \varphi_{U^{j+1}_2} - \varphi_{U^{j+1}_4}\right),\\
{}^1\Psi^2_{F^l_{j+1},\,U^j} &= \frac{1}{6}\left(\varphi_{U^{j+1}_1} + \varphi_{U^{j+1}_3} + 3\varphi_{U^{j+1}_2} - 5\varphi_{U^{j+1}_4}\right),\\
{}^2\Psi^1_{F^l_{j+1},\,U^j} &= \frac{1}{2}\left(\varphi_{U^{j+1}_1} + \varphi_{U^{j+1}_3} - \varphi_{U^{j+1}_2} - \varphi_{U^{j+1}_4}\right),\\
{}^2\Psi^2_{F^l_{j+1},\,U^j} &= -\frac{1}{6}\left(\varphi_{U^{j+1}_1} + \varphi_{U^{j+1}_3} + 3\varphi_{U^{j+1}_2} - 5\varphi_{U^{j+1}_4}\right),
\end{aligned}
$$

for $l = 1$ and similarly for $l = 2, 3$. These wavelets are exactly the wavelets obtained in [2], in the case when the spherical areas are approximated with the plane areas.

4 The stability of the bases

To be useful in practice, the wavelets must satisfy the Riesz stability conditions. Next we prove the Riesz stability of the bases that we have constructed in V^j and W^j, for arbitrary $j \in \mathbb{N}$.

First we check the condition 3 of the definition of multiresolution. The basis $\left\{2^j\varphi_{U^j_k},\ k = 1, 2, \ldots, n \cdot 4^j\right\}$ of V^j is orthonormal since

$$
\left\|2^j\varphi_{U^j_k}\right\|^2_* = 4^j\left\langle\varphi_{U^j_k}, \varphi_{U^j_k}\right\rangle_* = 4^j \cdot \frac{a\left(p^{-1}\left(U^j_k\right)\right)}{a\left(p^{-1}\left(U\right)\right)} = 1
$$

and $\left\langle 2^j\varphi_{U^j_k}, 2^j\varphi_{U^j_l}\right\rangle_* = 0$ for $k \neq l$ because the intersection of their supports is either empty or an edge, which has the measure zero.

Being an orthonormal basis with respect to the inner product $\langle\cdot,\cdot\rangle_*$, the following equality holds

$$
\left\|\sum_{U^j\in\mathcal{U}^j} c^j_U 2^j\varphi_{U^j}\right\|_* = \left\|\left\{c^j_U\right\}_{U\in\mathcal{U}^j}\right\|_{l^2}.
$$

Using now the equality (3) , which expresses the equivalence of the norms $\|\cdot\|_*$ and $\|\cdot\|_{L^2(\mathbb{S}^2)}$, we get

$$\frac{1}{M}\left\|\left\{c_U^j\right\}_{U\in\mathcal{U}^j}\right\|_{l^2}^2 \leq \left\|\sum_{U^j\in\mathcal{U}^j} c_U^j 2^j \varphi_{U^j}\right\|_{L^2(\mathbb{S}^2)}^2 \leq \frac{1}{m}\left\|\left\{c_U^j\right\}_{U\in\mathcal{U}^j}\right\|_{l^2}^2,$$

which is exactly the condition 3 of the definition of a multiresolution.

Using the same arguments for the wavelets bases $\left\{2^j\,{}^{\mathbf{i}}\Psi^{\mathbf{k}}_{F^l_{j+1},U^j}\right\}_{l=1,2,3,\ U^j\in\mathcal{U}^j}$, $\mathbf{i}=1,2,\ \mathbf{k}=1,2$, we can prove that

$$\frac{1}{M}\left(\sum_{l=1}^{3}\sum_{U\in\mathcal{U}^j} d_{l,U^j}\right)^2 \leq \left\|\sum_{U^j\in\mathcal{U}^j} d_{l,U^j} 2^j\,{}^{\mathbf{i}}\Psi^{\mathbf{k}}_{F^l_{j+1},U^j}\right\|_{L^2(\mathbb{S}^2)}^2 \leq \frac{1}{m}\left(\sum_{l=1}^{3}\sum_{U\in\mathcal{U}^j} d_{l,U^j}\right)^2.$$

Some evaluations of the number $\kappa=\sqrt{M/m}$ for some particular polyhedrons shows that κ is $3^{3/2}=5.19615\ldots$ for the regular tetrahedron, $3^{3/4}=2.27951\ldots$ for the cube and regular octahedron and $\left(15/(5+2\sqrt{5})\right)^{3/4}=1.41167\ldots$ for the regular dodecahedron and regular icosahedron. However, the number κ is not significant for the performance of the wavelets, since the matrices involved in the decomposition and reconstruction algorithms are orthogonal.

5 Numerical tests

In order to illustrate our wavelets, we took as the initial polyhedron Π an octahedron with six vertices and we performed five levels of decomposition. At the level five, the total number of triangles is 8196. Then we considered a particular data set *pol*5 from texture analysis of crystals (cf. [4]) and we represented it in Figure 4. It consists of 36×72 measurements on the sphere at the points

$$\{P_{ij}\left(\cos\theta_j\sin\rho_i,\sin\theta_j\sin\rho_i,\cos\rho_i\right)\},$$

with $\theta_j=\frac{\pi j}{36}-\frac{\pi}{72},\ j=1,\ldots,72,\ \rho_i=\frac{\pi i}{36}-\frac{\pi}{72},\ i=1,\ldots 36$. Its main characteristic is that the values over the whole sphere are constant, except for some peaks. First we have approximated this data with the function $f^5\in V^5$(see figure 5), considering *pol*5 as a piecewise constant function on the set

$$\{p(\mathcal{Q}_{ij}),\ i=1,\ldots 36,\ j=1,\ldots 72,\},$$

where p is the projection defined in (1) and $\mathcal{Q}_{ij}$ are quadrates with centers at P_{ij} and edge $\pi/72$. The approximation error

$$e=\frac{1}{36\cdot 72}\sum_{i=1}^{36}\sum_{j=1}^{72}\left|f^5(i,j)-pol5(i,j)\right|$$

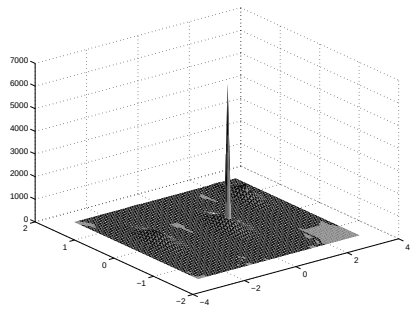

Fig. 4. The initial data set *pol*5

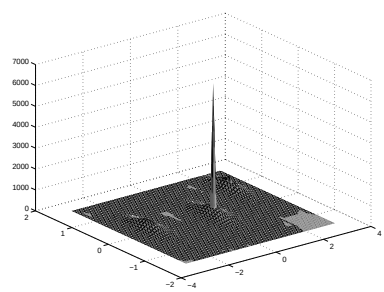

Fig. 5. The function $f^5 \in \mathcal{V}^5$, approximation of *pol*5 at the level 5.

was 1.0984. Since the set $\left\{\varphi_t^j\right\}_{t\in\mathcal{U}^j}$ is a basis for V^j, for $j = 0, 1, 2, \ldots$, we can write

$$f^5(\eta) = \sum_{t\in\mathcal{U}^5} f_t^5 \varphi_t^5(\eta), \ \eta \in \mathbb{S}^2. \tag{11}$$

The vector $\mathbf{f}^5 = \left(f_t^5\right)_{t\in\mathcal{U}^5}$ associated to the function f^5 was then decomposed into $\mathbf{f}^0$ and $\mathbf{g}^0$, $\mathbf{g}^1$, $\mathbf{g}^2$, $\mathbf{g}^3$, $\mathbf{g}^4$, using the wavelet with coefficients $(\alpha_1, \alpha_2, \beta, \gamma) = \left(\frac{1}{6}, \frac{1}{6}, \frac{3}{6}, -\frac{5}{6}\right)$. The details coefficients $\mathbf{g}^j$, $j = 0, \ldots, 4$ were thresholded to obtain a specific compression rate. More precise, their components $\left(g_k^j\right)_{k=1,\ldots,3n\cdot 4^j}$ were replaced with the values $\left(\widehat{g}_k^j\right)_{k=1,\ldots,3n\cdot 4^j}$ according to a strategy known as *hard thresholding.* This consist in choosing a threshold $\varepsilon > 0$ and then setting

$$\widehat{g}_k^j = \begin{cases} g_k^j, \text{ if } \left|g_k^j\right| \geq \varepsilon, \\ 0, \quad \text{otherwise.} \end{cases}$$

The ratio of the number of subsequent non-zero coefficients to the total number,

$$\frac{\sum_{j=0}^{4} \left|\left\{k : \widehat{g}_k^j \neq 0\right\}\right|}{3n \cdot 4^j}$$

will be referred to as the *compression rate.*

After the compression we performed the reconstruction, yielding an approximation with error $\mathbf{e}^5$, $\mathbf{e}^5 = \mathbf{f}^5 - \widehat{\mathbf{f}}^5$, where $\widehat{\mathbf{f}}^5 = \left(\widehat{f}_t^5\right)_{t\in\mathcal{U}^5}$ is the vector associated to the reconstructed function $\widehat{f}^5$. We have measured this error in several ways:

- The maximum error given by

$$\left\|\mathbf{e}^5\right\|_\infty = \max_{\eta\in\mathbb{S}^2}\left|\mathbf{e}^5(\eta)\right| = \max_{t\in\mathcal{U}^5}\left|\mathbf{e}_t^5\right|;$$

- The 2−norm

$$\left\|\mathbf{e}^5\right\|_2 = \left(\sum_{t\in\mathcal{U}^5}\left|f_t^5 - \widehat{f}_t^5\right|^2\right)^{1/2};$$

- The mean absolute error over the triangles

$$\text{mean}\left(\mathbf{e}^5\right) = \frac{1}{n\cdot 4^j}\sum_{t\in\mathcal{U}^5}\left|\mathbf{e}_t^5\right|.$$

Figures 6, 7 and 8 show the reconstructed functions $\widehat{f}^5$ for different compression rates, and the errors are tabulated in Table 1.

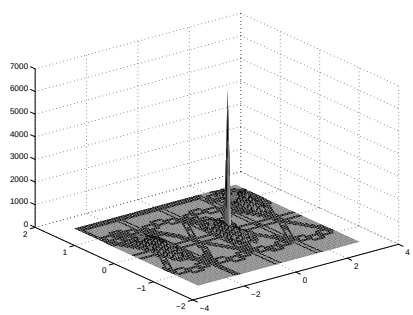

Fig. 6. The reconstructed function $\widehat{f}^5$ for the compression rate 0.05.

References

1. Bonneau, G-P.: Optimal Triangular Haar Bases for Spherical Data. In: IEEE Visualization '99, San Francisco, USA (1999).
2. Nielson, G., Jung, I., Sung, J.: Haar Wavelets over Triangular Domains with Applications to Multiresolution Models for Flow over a Sphere. In: IEEE Visualization '97, 143-150 (1997).
3. Roşca, D.: Locally Supported Rational Spline Wavelets on the Sphere, submitted.
4. Schaeben, H., Potts, D., Prestin, J.: Spherical Wavelets with Application in Preferred Crystallographic Orientation, IAMG' 2001, Cancun (2001).

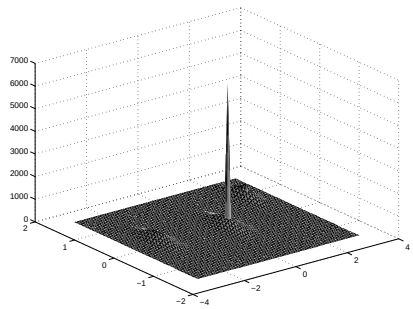

Fig. 7. The reconstructed function $\widehat{f}^5$ for the compression rate 0.5.

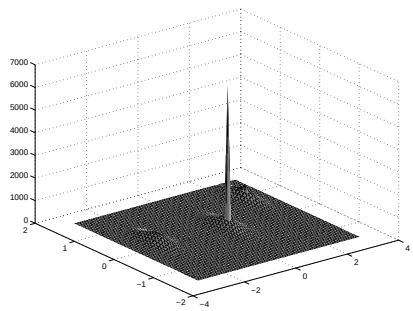

Fig. 8. The reconstructed function $\widehat{f}^5$ for the compression rate 0.75.

Table 1. Reconstruction errors for some compression rates, with the wavelet $\frac{1}{6}[1, 1, 3, -5]$

comp. rate	no. of zero coeff.	$\left\|\mathbf{e}^5\right\|_\infty$	$\left\|\mathbf{e}^5\right\|_2$	mean $\left(\mathbf{e}^5\right)$
0.05	7775	165.75	3122.10	29.40
0.1	7366	114.48	2715.90	25.13
0.25	6139	78.41	1855.40	15.48
0.5	4099	35.17	764.91	6.40
0.75	2047	19.24	242.26	1.53
0.8	1637	4.11	88.99	0.55
0.84	1228	0	0	0